

Structure of the exotic spin-flop states in $\text{BaCu}_2\text{Si}_2\text{O}_7$.

A. Zheludev,^{1,2,*} E. Ressouche,³ I. Tsukada,⁴ T. Masuda,⁵ and K. Uchinokura⁵

¹*Solid State Division, Oak Ridge national Laboratory, Oak Ridge, TN 37831-6393, USA.*

²*Previous address: Physics Department, Brookhaven National Laboratory, Upton, NY 11973, USA.*

³*DRFMC/SPSMS/MDN, CENG, 17 rue des Martyrs, 38054 Grenoble Cedex, France.*

⁴*Central Research Institute of Electric Power Industry,
2-11-1, Iwato kita, Komae-shi, Tokyo 201-8511, Japan*

⁵*Department of Advanced Materials Science, The University of Tokyo,
6th Engineering Bldg., 7-3-1 Hongo, Bunkyo-ku, Tokyo 113-8656, Japan*

(Dated: August 24, 2021)

The unusual 2-stage spin flop transition in $\text{BaCu}_2\text{Si}_2\text{O}_7$ is studied by single-crystal neutron diffraction. The magnetic structures of the various spin-flop phases are determined. The results appear to be inconsistent with the previously proposed theoretical explanation of the 2-stage transition.

I. INTRODUCTION

The quasi-one-dimensional (quasi-1D) $S = 1/2$ antiferromagnet $\text{BaCu}_2\text{Si}_2\text{O}_7$ is recognized as an almost ideal model material for studying exotic spin dynamics in weakly-interacting quantum spin chains.¹ In a series of papers^{2,3,4} we have demonstrated that in this compound it is possible to observe a separation between single-particle spin wave excitations, characteristic of a classical system with long-range magnetic order, and a gapped continuum of states that is a property of the quantum 1D Heisenberg model. Quite recently however, another aspect of the physics of $\text{BaCu}_2\text{Si}_2\text{O}_7$ attracted a great deal of attention. It was found that in the ordered state of $\text{BaCu}_2\text{Si}_2\text{O}_7$, an application of a magnetic field along the direction of ordered moment leads to *two* consecutive spin re-orientation transitions.⁵ This phenomenon is in contrast with the typical behavior of a conventional antiferromagnet in a field, where only a single “spin-flop” transition occurs.

By far, the largest energy scale of magnetic interactions in $\text{BaCu}_2\text{Si}_2\text{O}_7$ is that of antiferromagnetic nearest-neighbor coupling within the spin chains, that run along the c axis of the orthorhombic crystal structure (space group $Pnma$, $a = 6.862(2)\text{Å}$, $b = 13.178(1)\text{Å}$ and $c = 6.897(1)\text{Å}$.⁶) The in-chain exchange constant is $J = 24.1\text{ meV}$, as previously determined from inelastic neutron scattering experiments and bulk susceptibility measurements.^{1,3} Exchange coupling between the chains is much weaker, with $J_x = -0.46\text{ meV}$ and $J_y = 0.20\text{ meV}$, for nearest-neighbors along the a and b axes, respectively, and $J_3 = 0.15\text{ meV}$ along the (110) diagonal.³ The spin wave spectrum shows a small anisotropy gap of about 0.3 meV , corresponding to an easy axis along the (001) crystallographic direction.³ Long-range magnetic ordering occurs at a low Néel temperature of $T_N \approx 9.2\text{ K}$.¹ The ordered magnetic moment is rather small, $m_0 = 0.15\ \mu_B$ per Cu^{2+} .^{2,3} In the ordered state the spins are parallel to the magnetic easy axis. Nearest-neighbor spins along the b and c axes are aligned antiparallel relative to each other, while nearest neighbors along a are ferromagnetically aligned.^{1,3} The

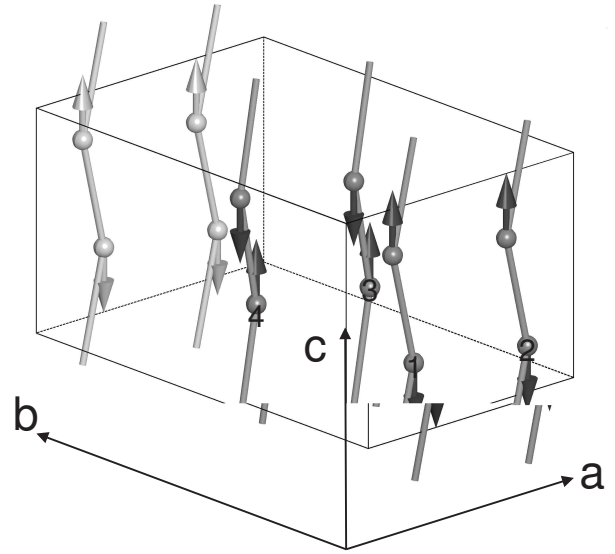


FIG. 1: A schematic view of the zero-field magnetic structure of $\text{BaCu}_2\text{Si}_2\text{O}_7$. The $S = 1/2$ Cu^{2+} ions form slightly zigzag antiferromagnetic chains.

spin structure is visualized in Fig. 1. The phase transitions that are the subject of this work occur at relatively low fields $H_{c1} = 2.0\text{ T}$ and $H_{c2} = 4.9\text{ T}$, applied along the easy axis, and produce characteristic jumps in the magnetization curve.⁵ To date, the spin structure in the high-field phases has not been determined. However, in Ref. 5 it was suggested that upon going through the first transition, the spins “flop” into the (a, b) crystallographic plane. The second transition was then described as an unusual *spin rotation within the plane perpendicular to the field*, and is somewhat similar to that recently found in $\text{K}_2\text{V}_3\text{O}_8$.⁷

Based on an analysis of the high-field magnetization data, it was conjectured⁵ that the unusual second spin re-orientation in $\text{BaCu}_2\text{Si}_2\text{O}_7$ is a result of competition between Dzyaloshinskii-Moriya (DM) off-diagonal exchange interaction in the spin chains and isotropic exchange cou-

pling between the chains. In the present work we report the results of magnetic neutron diffraction studies of the various spin-flop states in $\text{BaCu}_2\text{Si}_2\text{O}_7$. We find the results to be *inconsistent with the previously proposed model*. It appears that inter-chain coupling dominates over DM interactions, and that the series of spin re-orientation transitions can not result from a competition between the two effects alone. Alternative mechanisms for the two-stage spin flop transition in $\text{BaCu}_2\text{Si}_2\text{O}_7$ are discussed.

II. EXPERIMENTAL

A $5 \times 5 \times 4 \text{ mm}^3$ sample was mounted in a 6 T cryomagnet on the D23 lifting counter diffractometer at Institut Laue Langevin. The $(0, 0, 1)$ axis was aligned parallel to the field direction. With 8 magnetic Cu^{2+} per unit cell, in the ordered state all magnetic reflections coincide with nuclear ones. In addition, the ordered magnetic moment in $\text{BaCu}_2\text{Si}_2\text{O}_7$ is small, and detecting the magnetic contributions to Bragg intensities is rather difficult. The measurements were therefore performed in differential mode. At $H = 0 \text{ T}$, 4 T (below H_{c2}) and 5 T (above H_{c2}) the diffractometer was consecutively positioned on each accessible Bragg reflection. Without moving any instrument motors, the peak intensity was measured first at 2 K and then again at 10 K. This measurement yielded the ratio of nuclear and magnetic scattering intensities. The absolute values of nuclear intensities were separately measured at 10 K in standard rocking scans. The rocking curves also provided an estimate of the background around each Bragg position. The measured integrated nuclear intensities, backgrounds, and peak intensity ratios were then used to estimate integrated magnetic intensities. In another experiment, the peak intensities of $(41\bar{1})$, $(03\bar{1})$ and $(05\bar{1})$ reflections were monitored as a function of applied field in the range 0–5.5 T. Peak intensities measured in this fashion were assumed to be proportional to integrated intensities, with the normalization factor determined at $H = 0$, as described above.

III. RESULTS

Due to the strong in-chain coupling, any canting of neighboring spins away from a perfect antiferromagnetic alignment within each chain will be small and undetectable in our measurements. In analyzing the data, we could therefore safely rely on an approximation in which within each chain all spins are collinear. Inter-chain coupling is considerably weaker than the in-chain one, and is comparable in strength to the Zeeman energy associated with experimental fields. For this reason the relative orientation of staggered moments in neighboring chains could not be considered fixed, as it may actually vary with field. Since there are four chains within each unit cell of $\text{BaCu}_2\text{Si}_2\text{O}_7$, solving the magnetic structure

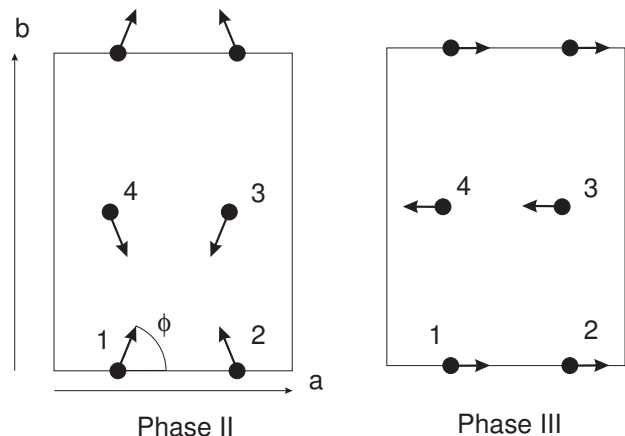


FIG. 2: A model for the spin arrangement in $\text{BaCu}_2\text{Si}_2\text{O}_7$ in magnetic fields applied along the c axis: Phase II for $2 \text{ T} = H_{c1} < H < H_{c2} = 4.7 \text{ T}$ and Phase III for $H > H_{c2}$. The spins are largely confined to the (a, b) crystallographic plane.

at each field was reduced to determining the orientations of four spins, one from each chain, labeled as \mathbf{S}_1 – \mathbf{S}_4 in Fig. 1.

A. Spin structure at zero applied field: Phase I

As a first step, we have verified that our new data collected at $H = 0$ are consistent with the structure previously reported in Ref. 3. The spins are parallel to the c -axis, with nearest neighbor spins along the c and b axes antiparallel to each other, and a parallel alignment of nearest neighbor spins along the a axis, as shown in Fig. 1. This type of spin arrangement minimizes all inter-chain interaction energies that were independently measured using inelastic neutron scattering.³ Magnetic Bragg intensities calculated for this c -axis collinear state are in good agreement with those measured at $H = 0$ in the present work. This comparison is made in Table I.

B. Spin structure at $H = 4 \text{ T}$: Phase II

The magnetic structure at $H = 4 \text{ T}$ was solved using a reverse Monte Carlo analysis, which unambiguously pointed to a planar state with all spins in the (a, b) plane and a canting by an angle $\phi \approx 80^\circ$, as shown in Fig. 2 on the left. This structure is a slight distortion of a collinear one, with all spins parallel to the b axis, and the same relative alignment of spins in adjacent chains as at $H = 0$. A least-squares refinement of the canting angle and the ordered moment then yielded $\phi = 78(3)^\circ$, $m_0 = 0.18(2) \mu_B$, with a residual $\chi^2 = 2.4$. A comparison between measured and calculated magnetic intensities is given in Table II. Assuming $\phi = 90^\circ$ (b -axis collinear state), one can still get a reasonably good agreement with experiment, with $\chi^2 = 2.8$. Note that the magnetic

TABLE I: Measured magnetic intensities at $H = 0$ in comparison to those calculated for the c -axis colinear state visualized in Fig. 1.

h	k	l	I_{calc}	I_{obs}	σ_{obs}	$\frac{I_{\text{obs}} - I_{\text{calc}}}{\sigma_{\text{obs}}}$
3	-5	-1	1.073	0.014	0.349	-3.034
-1	3	-1	2.434	2.066	0.588	-0.625
-1	-3	-1	2.547	3.574	0.605	1.697
-1	-2	-1	0.000	0.149	0.942	0.158
-3	2	-1	0.002	0.951	0.973	0.975
4	1	0	19.980	19.116	1.010	-0.855
1	-3	-1	2.547	4.038	1.015	1.469
-4	1	0	19.980	20.973	1.111	0.894
-2	6	-1	0.093	0.741	1.114	0.582
-1	2	-1	0.000	2.889	1.163	2.484
1	-1	-1	1.886	2.468	1.173	0.496
0	-6	0	0.797	1.565	1.191	0.644
-1	-1	-1	1.886	3.357	0.856	1.719
-1	1	-1	1.789	4.262	1.260	1.963
0	4	0	0.527	2.109	1.352	1.170
0	-3	-1	38.129	35.631	1.080	-2.313
-3	-2	-1	0.002	1.162	1.660	0.699
-2	1	0	10.223	10.306	1.264	0.066
0	-5	-1	33.209	39.198	1.277	4.689
-3	-5	-1	1.073	3.024	1.804	1.081
-2	-1	0	10.223	9.102	1.829	-0.613
1	-7	-1	1.421	0.974	1.341	-0.333
-3	5	-1	1.053	2.096	1.854	0.562
-2	0	0	0.000	3.193	1.897	1.683
2	-4	-1	0.058	0.306	2.009	0.123
-2	4	-1	0.057	1.714	2.106	0.787
-1	-7	-1	1.421	1.277	2.166	-0.066
-2	-4	-1	0.058	7.373	2.227	3.284
2	-7	-1	15.898	16.154	2.626	0.098

$\chi^2 = 2.8$

structure of Phase II proposed in Ref. 1 (all spins parallel or antiparallel to the a -axis) is totally inconsistent with the present experiment, corresponding to $\chi^2 = 64$, even when m_0 is optimized to best fit the data.

C. Spin structure at $H = 5$ T: Phase III.

Fewer data points were collected at $H = 5$ T than for the other two field values (see Table III). The best agreement with the data was obtained assuming a collinear structure with all spins pointing along the a axis (Fig. 2, right), and the same relative alignment of spins in adjacent chains as at $H = 0$. The refined value for the ordered moment is $m_0 = 0.17(2) \mu_B$, and for this model $\chi^2 = 4.5$. Again we note that the spin arrangement proposed in Ref. 5 for the high-field phase (all spins along

TABLE II: Measured magnetic intensities at $H = 4$ T in comparison to those calculated for the canted state visualized in Fig. 2(left).

h	k	l	I_{calc}	I_{obs}	σ_{obs}	$\frac{I_{\text{obs}} - I_{\text{calc}}}{\sigma_{\text{obs}}}$
-4	1	0	14.048	13.239	0.635	-1.273
0	-6	0	0.000	0.170	1.210	0.140
-2	0	0	0.000	3.560	1.930	1.845
-2	1	0	6.126	10.760	1.750	2.648
4	1	0	14.048	15.720	0.990	1.689
-3	-5	-1	0.761	1.510	1.730	0.433
-4	-1	-1	21.136	20.890	1.340	-0.183
-1	-7	-1	0.185	2.260	2.100	0.988
-3	-2	-1	0.447	0.710	1.620	0.163
-1	-6	-1	1.417	1.390	0.760	-0.036
-4	1	-1	21.136	22.660	1.560	0.977
-1	-3	-1	1.487	0.730	0.800	-0.946
0	-5	-1	5.341	4.140	1.730	-0.694
-1	-1	-1	3.828	4.330	1.180	0.426
0	-3	-1	16.846	13.950	1.480	-1.957
2	-7	-1	4.127	1.300	2.540	-1.113
-3	5	-1	0.761	2.710	1.860	1.048
2	-6	-1	0.087	0.310	0.870	0.256
-1	1	-1	3.828	8.850	1.300	3.863
1	-3	-1	1.487	0.850	1.010	-0.631

$\chi^2 = 2.4$
 $m_0 = 0.18(2) \mu_B$
 $\phi = 78(3)^\circ$

the b axis and nearest-neighbor spins in the a direction aligned parallel to each other) is totally inconsistent with experiment, corresponding to $\chi^2 = 158$.

IV. FIELD DEPENDENCE.

The measured field dependencies of $(\bar{4}1\bar{1})$, $(0\bar{3}\bar{1})$ and $(0\bar{5}\bar{1})$ reflections are shown in Fig. 3. The data for Phases II and III were analyzed using the established models. The value of magnetic moment m_0 , as well as the canting angle ϕ for Phase II were refined to best-fit the three intensities at each field. The results of the fit are shown in solid lines in Fig. 3, and the field dependence of the fit parameters is plotted in Fig. 4.

To obtain a good fit to the field dependencies measured in Phase I, an additional parameter had to be introduced to account for the large change in intensities just below the phase transition at H_{c1} . By trial and error, it was found that the best way to reproduce this effect is to assume that the spin structure, as a whole, tilts towards the b axis (Fig. 5). In this model, when the direction of staggered moment passes through the $(0\bar{3}\bar{1})$ direction, the corresponding Bragg intensity shows a characteristic dip (arrow in Fig. 3a). This behavior is a result of

TABLE III: Measured magnetic intensities at $H = 5$ T in comparison to those calculated for the a -axis colinear state visualized in Fig. 2 (right).

h	k	l	I_{calc}	I_{obs}	σ_{obs}	$\frac{I_{\text{obs}} - I_{\text{calc}}}{\sigma_{\text{obs}}}$
-4	1	0	0.845	0.110	0.890	-0.826
-4	-1	-1	1.562	2.030	1.200	0.390
-4	1	-1	1.562	4.570	1.470	2.046
-1	-3	-1	3.655	2.268	0.408	-3.396
0	-5	-1	49.258	54.301	1.672	3.016
-1	-1	-1	3.460	3.342	0.498	-0.237
0	-3	-1	68.598	61.640	2.690	-2.587
-1	1	-1	3.460	5.706	0.876	2.562
1	-3	-1	3.655	2.200	0.725	-2.008
-1	-6	-1	0.003	0.377	0.445	0.838

$\chi^2 = 4.5$
 $m_0 = 0.17(2) \mu_B$

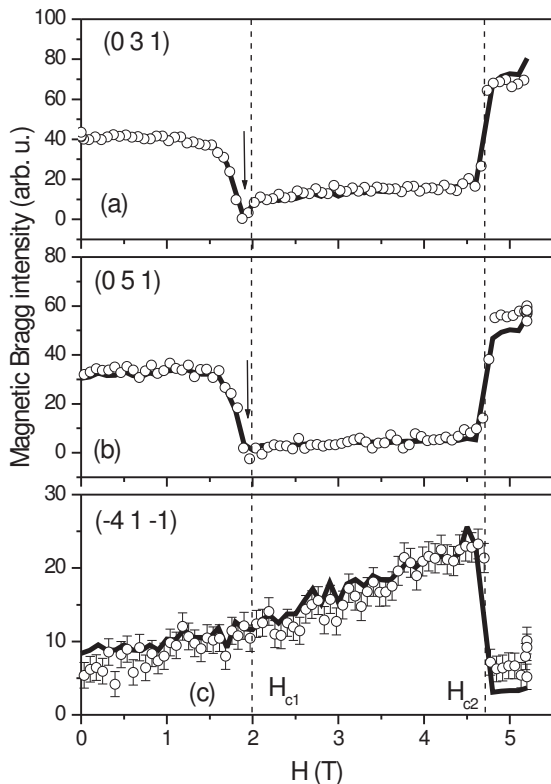


FIG. 3: Measured field dependencies of several magnetic Bragg reflections in $\text{BaCu}_2\text{Si}_2\text{O}_7$ (symbols). The solid lines are a fit to the data at each field using the models described in the text. The arrows indicate intensity dips just below the phase transition at H_{c1} .

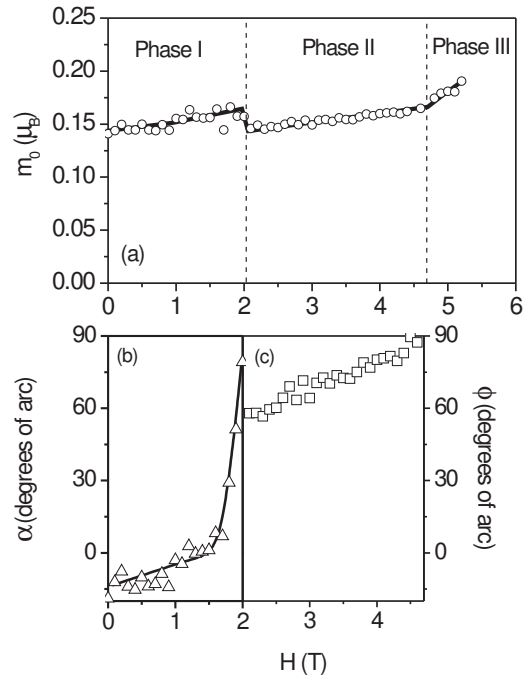


FIG. 4: Symbols: Measured field dependence of ordered moment (a), tilt angle α in Phase I (b) and canting angle ϕ in Phase II (c). The solid lines are a guide for the eye.

the neutron polarization intensity factor going to zero for scattering vectors that are parallel to ordered magnetic moment. A smaller dip, at a slightly larger field is seen in the (051) peak as well (arrow in Fig. 3b). By varying m_0 and the tilt angle α , a good fit to the data collected at $0 < H < H_{c1}$ could be obtained. The result of the fit is shown in solid lines in Fig. 3, and the field dependence of the fit parameters is plotted in Fig. 4. Note that the angle α is shown as negative at small fields. In fact, the tilt α probably remains close to zero and positive, except immediately before the transition, where it rapidly increases to 90° . The negative values obtained in the fit are an artifact of using only three measured intensities in the analysis. For small α the experiment is fairly insensitive to this parameter, due to a $\cos^2 \alpha$ term in the intrinsic polarization factor for the scattering cross section and the fact that all data were collected close to the (001) reciprocal-space plane. However, as α approaches 90° , the polarization sensitivity is greatly enhanced.

V. DISCUSSION

The data analysis described above was based on the known room-temperature crystal structure. The use of room-temperature structure factors to determine spin orientations at low temperatures may lead to systematic errors. Additional errors may be associated with measur-

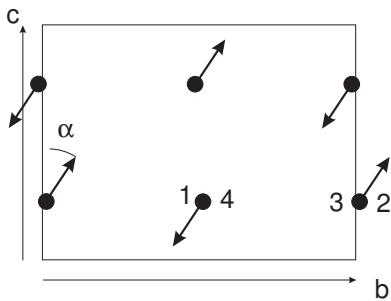


FIG. 5: Tilting of the spin structure in $\text{BaCu}_2\text{Si}_2\text{O}_7$ in magnetic fields $H < H_{c1} = 2$ T, applied along the c axis (Phase I). The spins are largely confined to the (b, c) crystallographic plane.

ing magnetic intensities in the temperature-differential mode. Nevertheless, the results allow us to establish the main features of the three phases: 1) Nearest-neighbor spins within each chain remain almost anti-parallel to each other at all times. 2) The relative alignment of adjacent spins from neighboring chains does not deviate significantly from that at $H = 0$, with ferromagnetic spin alignment along a and antiferromagnetic along b . Even in Phase II the canting is not very dramatic and vanishes just before the transition at H_{c2} . 3) The spins are oriented roughly along the c , b and a axis in phases I, II and III, respectively. 4) The ordered moment is only slightly field-dependent and remains close to $0.15\mu_B$.

In weakly coupled quantum spin chains the ordered moment m_0 is proportional to $\sqrt{|J_\perp|/J}$, where J_\perp is the effective mean-field inter-chain coupling strength.⁸ At $H = 0$ the structure is such that $|J_\perp| = J_b + 2J_3 + |J_a|$.³ The fact that m_0 remains practically constant when going through the phase transitions, means that in Phases II and III, J_\perp does not change much and nearest-neighbor spins remain close to being parallel to one another along the a axis and antiparallel along the b and c directions. This can be seen as an important self-consistency check for our determination of the spin orientations in the three phases. The overall gradual increase of the ordered moment as a function of H seen in Fig. 4a is to be expected, and is due to the suppression of 1D quantum spin fluctuations by the symmetry-breaking external field. The slight suppression of m_0 observed in Phase II (Fig. 4a) is a result of the canted geometry, in which $|J_\perp|$ is reduced compared to that in Phase I. In the presence of canting ($\phi < 90^\circ$) the effective inter-chain coupling is given by $|J_\perp| = 2J_3 - (J_b + |J_a|)\cos(2\phi)$. In particular, just above H_{c1} , $\phi = 60^\circ$, and the drop in m_0 expected on going through the first phase transition due to the abrupt change in $|J_\perp|$ is about 23%. This value is in reasonable agreement with the observed $\approx 15\%$ effect.

Given the available data, the spin re-orientation at H_{c1} can be described as a more or less conventional spin-flop transition, that one expects for a classical antiferromagnet in a magnetic field applied along the easy axis. In zero field, the easy- c -axis anisotropy energy is minimized

when all spins are perpendicular to the (a, b) plane. To take advantage of the Zeeman energy in applied fields, the spins have to align themselves perpendicular to c , to allow a canting of the rigid antiferromagnetic structure in the direction of \mathbf{H} . Dzyaloshinskii-Moriya interactions and inter-chain coupling may modify the transition field and produce the small canting found in Phase II, but do not affect the basic physics of the effect. The fact that the transition appears to have a precursor, the spin structure tilting by an angle α at $H < H_{c1}$, may have several explanations. One possibility is that this phenomenon is result of an imperfect alignment of the external magnetic field relative to the c axis of the crystal. Alternatively, it can be an intrinsic effect, due to the presence of Dzyaloshinskii-Moriya interaction, or to the existing structural canting of the local anisotropy axes of Cu^{2+} relative to the c axis. To fully resolve this problem, a careful determination of the magnetic structure just below and just above H_{c1} will be required.

The second phase transition is much more unusual, since it involves a spin rotation in the plane perpendicular to \mathbf{H} . It is clear that such behavior requires the presence of off-diagonal exchange interactions in the system. As recently observed in $\text{K}_2\text{V}_3\text{O}_8$, for example, a spin rotation around the field direction can be caused by a competition between DM interactions and magnetic anisotropy.⁷ This type of behavior is known since earlier studies of hematite.⁹ For $\text{BaCu}_2\text{Si}_2\text{O}_7$ though, a totally different explanation was proposed in Ref. 5, and the transition was attributed to a competition between DM coupling in the chains and isotropic inter-chain interactions, a mechanism similar to that previously discussed in relevance to the anomalous spin-flop behavior of La_2CuO_4 .¹⁰

The key argument of Ref. 5 is that the main components of the Dzyaloshinskii vector for the nearest-neighbor bond within the chains lie in the (a, b) plane, and alternate sign from one bond to the next. In this case, DM interactions produce a weak-ferromagnetic canting of the spins within each chain even in zero applied field. In the presence of an external field, additional canting is due to Zeeman energy. The free energy of the system is minimized when the two canting effects are in the same direction. For this to be the case, nearest-neighbor spins along the a axis have to be almost *antiparallel* to each other, since Dzyaloshinskii vectors in the adjacent chains are *antiparallel* as well. This preferred antiparallel orientation is in competition with *ferromagnetic* inter-chain coupling along the a axis. In the model proposed in Ref. 5, the frustration is resolved in Phase II by having all spins aligned almost parallel to the Dzyaloshinskii vector (roughly along the a axis), which practically eliminates the Dzyaloshinskii energy altogether, and the ferromagnetic inter-chain coupling energy along the a axis is minimized. In Phase III the model predicts that the combination of DM and Zeeman energies wins over inter-chain interactions: the spins rotate to be almost parallel to the b axis and cant in the direction of the applied field

to minimize both energies. At the same time, nearest-neighbors along the a axis become almost antiparallel, despite a ferromagnetic coupling in this direction.

The results presented above clearly demonstrate that the actual spin arrangements in $\text{BaCu}_2\text{Si}_2\text{O}_7$ in Phases II and III are totally different from those previously conjectured. In Ref. 5 it was emphasized that the Dzyaloshinskii vectors not being strictly parallel to the a axis, and additional inter-chain interactions along the $(0, 1, 0)$ and $(1, 1, 0)$ directions being present, the critical field and the details of the spin structures may deviate from those predicted by the simplified model. However, even in the more general case, if the H_{c2} transition in $\text{BaCu}_2\text{Si}_2\text{O}_7$ was indeed driven by a competition between DM interactions and isotropic inter-chain coupling, the energy of the latter would have to change abruptly upon going through the transition. The present data clearly show that this is *not* the case, since at H_{c2} the spin structure rotates as a whole, and the relative spin orientations, and with them the inter-chain exchange energies, remain practically unchanged. It appears that inter-chain coupling dominates over DM interactions in all three phases. Because of the canting in Phase II, the energy of inter-chain interactions is actually better minimized in Phase III, rather than Phase II. This sequence is opposite to that emerging from the model proposed in Ref. 5.

We believe that at the present stage it is unwise to attempt a quantitative explanation of the phase transitions in $\text{BaCu}_2\text{Si}_2\text{O}_7$ based on some specific spin Hamiltonian. Too many parameters are involved to make such an analysis unambiguous. The energy scale of inter-chain interactions and c -axis anisotropy are indeed similar to that defined by transition fields. However, the Hamiltonian is expected to have other terms on the same energy scale, and these *can not be dismissed*. In particular, measurements of the spin wave spectrum con-

tain evidence of an in-plane anisotropy of the magnitude ≈ 0.15 meV. This anisotropy is most likely due to the so-called Kaplan Schekhtman Entin-Wohlman Aharony (KSEA) interactions.¹¹ The KSEA term is a companion to DM interactions, and is an easy axis parallel to the Dzyaloshinskii vector. KSEA interactions are believed to be the driving force in the spin reorientation transition in $\text{K}_2\text{V}_3\text{O}_8$.⁷ The similarity of the behavior of the latter compound with that found in $\text{BaCu}_2\text{Si}_2\text{O}_7$ may indicate that anisotropy effects, and KSEA interactions in particular, could be responsible for the H_{c2} transition in the silicate as well.

VI. CONCLUSION

In summary, the actual mechanism of the exotic two-stage spin flop transition in $\text{BaCu}_2\text{Si}_2\text{O}_7$ remains a mystery. What is clear though, is that DM interactions and inter-chain exchange coupling alone can not sufficient to explain phenomenon. It appears more likely that both transitions in $\text{BaCu}_2\text{Si}_2\text{O}_7$ are caused by a competition between DM interactions and diagonal magnetic anisotropy effects, of which more needs to be learned.

Acknowledgments

One of the authors (I. T.) thanks J. Takeya for useful discussions. This work is supported in part by the Grant-in-Aid for COE Research ‘‘SCP coupled system’’ of the Japanese Ministry of Education, Science, Sports, and Culture. Oak Ridge National Laboratory is managed by UT-Battelle, LLC for the U.S. Department of Energy under contract DE-AC05-00OR22725.

* zhelud@bigfoot.com

¹ I. Tsukada, Y. Sasago, K. Uchinokura, A. Zheludev, S. Maslov, G. Shirane, K. Kakurai, and E. Ressouche, Phys. Rev. B **60**, 6601 (1999).

² A. Zheludev, M. Kenzelmann, S. Raymond, E. Ressouche, T. Masuda, K. Kakurai, S. Maslov, I. Tsukada, K. Uchinokura, and A. Wildes, Phys. Rev. Lett. **85**, 4799 (2000).

³ M. Kenzelmann, A. Zheludev, S. Raymond, E. Ressouche, T. Masuda, P. Boeni, K. Kakurai, I. Tsukada, K. Uchinokura, and R. Coldea, Phys. Rev. B **64**, 054422 (2001).

⁴ A. Zheludev, M. Kenzelmann, S. Raymond, T. Masuda, K. Uchinokura, and S.-H. Lee, Phys. Rev. B **65**, 014402 (2002).

⁵ I. Tsukada, J. Takeya, T. Masuda, and K. Uchinokura, Phys. Rev. Lett. **87**, 127203 (2001).

⁶ J. A. S. Oliveira, Ph.D. thesis, Ruprecht-Karls-Universitat, Heidelberg, 1993.

⁷ M. D. Lumsden, B. C. Sales, D. Mandrus, S. E. Nagler, and J. R. Thompson, Phys. Rev. Lett. **86**, 159 (2001).

⁸ H. J. Schulz, Phys. Rev. Lett. **77**, 2790 (1996).

⁹ For a theoretical discussion of spin reorientation transitions in easy-axis antiferromagnets with DM interactions see V. I. Ozhigin and V. G. Shapiro, Sov. Phys. JETP, **27**, 54 (1969); A. N. Bogdanov, Sov. J. Low Temp. Phys. **12**, 290 (1986), and references therein.

¹⁰ T. Thio, C. Y. Chen, B. S. Freer, D. R. Gabbe, H. P. Jenssen, M. A. Kastner, P. J. Picone, N. W. Preyer, and R. J. Birgeneau, Phys. Rev. B **41**, 231 (1990).

¹¹ T. A. Kaplan, Z. Phys. B **49**, 313 (1983); L. Shekhtman, O. Entin-Wohlman, and A. Aharony, Phys. Rev. Lett. **69**, 836 (1992); A. Zheludev, S. Maslov, G. Shirane, I. Tsukada, T. Masuda, K. Uchinokura, I. Zaliznyak, R. Erwin, L. P. Regnault, Phys. Rev. Lett. **81**, 5410 (1998).